

High pressure effect on molecular motions in the paraelectric phase of a vinylidene fluoride and trifluoroethylene copolymer (70/30) studied by n.m.r.

Myriam Stock-Schweyer*, Bernard Meurer and Gilbert Weill

*Institut Charles Sadron (CRM-EAHP), CNRS-ULP, 6 rue Boussingault, 67083
Strasbourg Cedex, France*

(Received 14 January 1993; revised 2 August 1993)

The ^{19}F n.m.r. spin-lattice relaxation times in both the laboratory and the rotating frame have been measured in a 70/30 mol% random copolymer of vinylidene fluoride and trifluoroethylene, over a range of pressures from 0.1 to 200 MPa in the paraelectric phase. Molecular motions have been investigated in this condish phase, and correlation times were obtained as a function of pressure and temperature. Activation parameters have been determined and discussed in terms of a thermally activated model and compared with literature data.

(Keywords: vinylidene fluoride; trifluoroethylene; molecular motion)

INTRODUCTION

Ferroelectric copolymers of vinylidene fluoride (VF_2) and trifluoroethylene (TrFE) have been extensively studied because of the presence of a clear Curie point (T_C) above room temperature. The known structural, physical and electrical characteristics accompanying the ferro- to paraelectric transition have been recently reviewed by Furukawa¹. Changes in the chain conformation (random sequences of TG , \overline{TG} and TT units instead of all TT) induce this transition over a broad temperature range (where the phases coexist) and considerable thermal hysteresis is found^{2,3}. The conformation disorder of the paraelectric phase has been found to be dynamic in character^{2,4-6}. Molecular motions in this phase have been extensively studied by incoherent quasi-elastic neutron scattering⁷ and n.m.r.⁸.

Copolymers with 70% VF_2 content were chosen because of a high degree of crystallinity ($\approx 70\%$) and because the paraelectric phase extends over the largest temperature range (from the melting point, ~ 423 K, down to the T_C , ~ 350 K).

N.m.r. experiments at atmospheric pressure show the existence of rapid and anisotropic motions, operating in both the paraelectric crystalline and the intercrystalline amorphous phases. Spin-lattice relaxation time measurements as a function of frequency (ν) in the whole paraelectric phase were found to show a $\nu^{-1/2}$ behaviour. Such a dispersion law indicates a one-dimensional diffusion of conformational changes.

In spite of the large spectral density explored (5–300 MHz) no cut-off frequency has been observed. However, as any deviation to the above behaviour must increase at low temperatures (above T_C) and high

frequencies (above 300 MHz), one would expect to reach a cut-off if the range of the dynamical n.m.r. measurements could be extended. The temperature range available is limited by the T_C and the melting temperature. Pressure is also an important thermodynamical parameter, affecting crystal structure and physical properties. The effects of hydrostatic pressure on $\text{P}(\text{VF}_2\text{-TrFE})$ have already been reported⁹⁻¹². Important changes in the T_C and cell parameters occur.

The present work was undertaken in order to study how molecular motions are controlled by pressure in the $\text{P}(\text{VF}_2\text{-TrFE})$ 70/30 mol% paraelectric phase. We report ^{19}F n.m.r. spin-lattice relaxation times (both in the laboratory and the rotating frame), studied over a range of pressures from 0.1 to 200 MPa.

EXPERIMENTAL

Spectrometer

N.m.r. measurements were carried out on a Bruker SXP spectrometer with a V3601-1 Varian electromagnet, operating at 56.4 MHz (^{19}F). The resonance field H_0 was controlled within $2\ \mu\text{T}$ by a field frequency lock (Drush, n.m.r. gaussmeter and regulation unit TAO2). Pulses were generated by a Hewlett-Packard pattern generator (model 8175A). The digitization was performed with a Lecroy 6810-12 bits converter (accuracy 1/2000), whose sampling frequency could be varied. The signal was then averaged and treated on a IBM-PC compatible ACER 1100 microcomputer. Numerical computations were performed in ASYST.

The width of a $\pi/2$ pulse was $\sim 4\ \mu\text{s}$. Measurement of T_1 was accomplished by the inversion-recovery pulse sequence. Decays were followed for about five T_1 s. The free induction decay (f.i.d.) signal was digitalized with two

* To whom correspondence should be addressed

time-scales. For the $T_{1\rho}$ experiments, the ^{19}F spins were spin-locked by applying a $\pi/2$ pulse followed by a pulse of variable τ_ρ phase shifted by $\pi/2$. Measurements were made at two field strengths corresponding to the frequencies: $\nu_1 = 62.5$ and 11 kHz.

The spin-lattice relaxation decays were fitted by non-linear least square adjustments of three to five parameters to a sum of exponentials according to $A \exp(-B\tau) + C \exp(-D\tau) + E$. Functions with the shape $g(\tau) = A \exp[-(1/\sigma)(\tau/B)^\sigma]$, where $1 \leq \sigma \leq 2$, were adjusted on the f.i.d., by extrapolating the signal through the dead time of the receiver ($6 \mu\text{s}$) to the middle of the pulse (time origin of the f.i.d.).

Pressure cell

The high pressure cell was built using Berylco 25 according to reference 13. The chosen diameters (25 and 12 mm) allowed a working pressure of 300 MPa. The sample was immersed in the pressure transmitting fluid in the radio frequency coil (8 mm diameter, 10 mm length). Pressure was generated by a high pressure pump (Nova Swiss). Silicon oil was used for ^{19}F studies at 56.4 MHz. Pressure was measured with a strain gauge with an accuracy of $\pm 1\%$. The pressure bomb was heated by a flow of gas and placed in a Dewar flask (± 3 K stability).

Sample

The P(VDF-TrFE) 70/30 copolymer with a number-average molecular weight (M_n) of 55 000 and polydispersity (M_w/M_n) of 1.9, was provided by Atochem Co. (France).

The sample was melted at 433 K prior to the measurements, and then a pressure cycle up to 180 MPa and a temperature run up to the paraelectric phase were carried out in order to remove any possible stress in the specimen.

Measurement procedure

The experiments were carried out isothermally and with several pressure runs (heating and cooling). Because of the large heat capacity of the vessel, a waiting period of ~ 2 –3 h was systematically used. In the same way, with regards to measurement reproducibility, a waiting period of ~ 20 min was used for each pressure.

During the course of each pressure run (2–3 days) no significant deviation in temperature was observed.

RESULTS

The measurements taken on compression and decompression runs were found to be identical within experimental error ($< 2\%$). All the results are reported for the paraelectric phase. Because phases coexist around the T_C , the phase diagram obtained by neutron diffraction under high pressure shown in Figure 1 is taken into account¹⁴.

Spin-lattice relaxation times

Laboratory frame T_1 . Over the entire pressure and temperature range explored, the relaxation is monoexponential, which is in agreement with previous work⁸.

The T_1 data are plotted as a function of pressure for different isotherms in Figure 2. Except at low pressure and high temperature, all the plots are linear, presenting a shift with temperature. T_1 decreases with increasing pressure. The solid lines were obtained by least squares linear regression. For the two highest temperatures, only

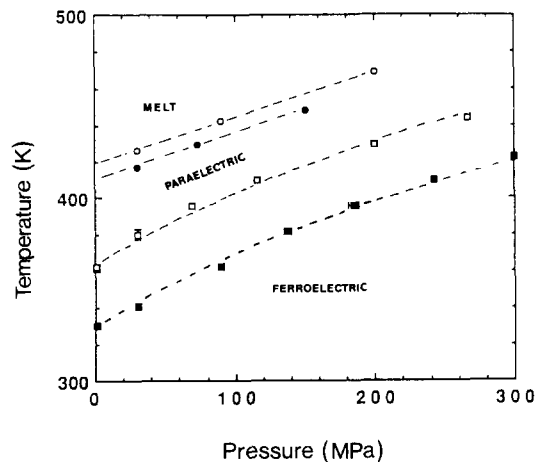


Figure 1 Phase diagram of a trifluoroethylene and vinylidene fluoride copolymer (70/30) obtained from neutron diffraction¹⁴; (\square , \blacksquare) Curie temperature on heating and cooling, respectively; (\circ , \bullet) melt and crystallization temperature, respectively

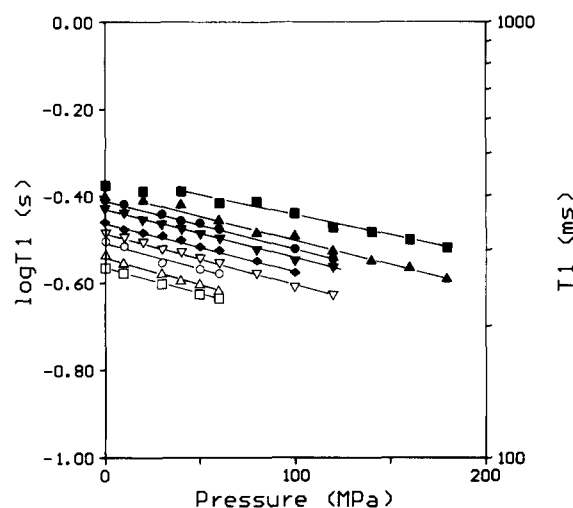


Figure 2 Experimental spin-lattice relaxation times T_1 as a function of pressure for different isotherms during the cooling run. Temperature (in K): (\blacksquare) 410; (\blacktriangle) 401; (\bullet) 398; (\blacktriangledown) 393.6; (\blacklozenge) 390.3; (∇) 386.2; (\circ) 383.6; (\triangle) 378; (\square) 374.6

the high pressure data were taken into account. The small deviation at low pressure may be due to premelting.

Rotating frame $T_{1\rho}$. For the three temperatures studied, the relaxation is monoexponential for $\nu_1 = 62.5$ kHz and appears to be biexponential for $\nu_1 = 11$ kHz over the entire pressure range. The two time constants differ by a factor of > 3 and the long component intensity represents $55 \pm 3\%$. An increase in pressure decreases the relaxation times (Figure 3).

As the relaxation was observed at two frequencies, plots of $(T_{1\rho})^{-1}$ and the 'total' $(T_1)^{-1}$ (at 62.5 kHz) satisfy a $(\nu_1)^{-1/2}$ behaviour (Figure 4). Nevertheless a deviation is observed at low temperature and high pressure.

F.i.d. analysis

Over the entire pressure and temperature range studied, the f.i.d. could be analysed in two components. An exponential ($\sigma = 1$) fitted the tail of the f.i.d. signal and a Gaussian ($\sigma = 2$) the beginning (the time constants were, respectively, ~ 100 and $28 \mu\text{s}$).

The proportion of Gaussian component was constant ($60 \pm 3\%$) over the entire temperature range studied in the

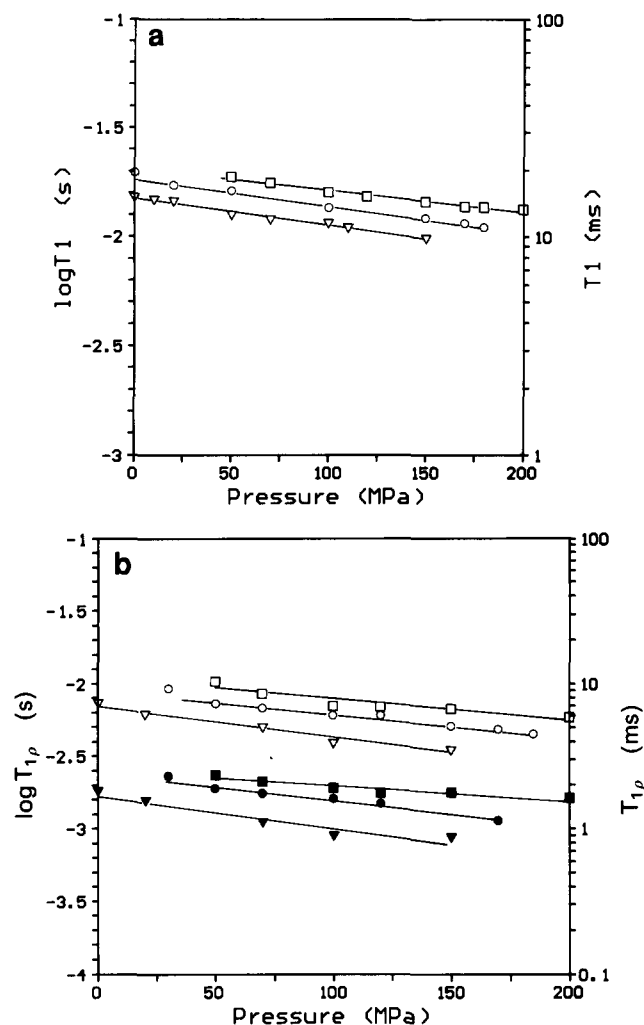


Figure 3 (a) Experimental spin-lattice relaxation times $T_{1\rho}$ (62.5 kHz) as a function of pressure for three isotherms: (□) 417; (○) 406; (▽) 390. (b) Measured $T_{1\rho}$ (11 kHz): open and solid symbols for the long and short component, respectively. The temperature symbols are the same as in (a)

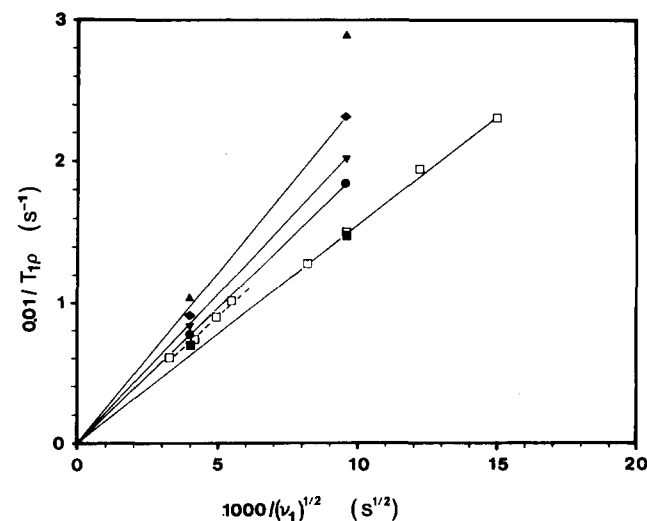


Figure 4 Plot of $(T_{1\rho})^{-1}$ versus $(\nu_1)^{-1/2}$ for different pressures at 390 K. Pressure (in MPa): (■) 0.1; (□) 0.1 (from ref. 3); (●) 50; (▼) 70; (◆) 100; (▲) 150

paraelectric phase. The Gaussian component represents the crystalline phase. Thus, the sample has a crystalline fraction of 60%. This value is lower than given by earlier determinations⁴ and than those found using other

techniques^{15,16}, but is in good agreement with the long component $T_{1\rho}$ intensity.

The second moment of the Gaussian component appears to be independent of pressure and temperature ($M_{2c} \approx 1.9 \text{ G}^2$). These results are in agreement with the proposed^{4,8} crystalline intramolecular origin of the observed M_2 and the pressure independence of the chain conformation¹⁴.

DISCUSSION

Our results are consistent with prior studies at atmospheric pressure⁸. Monoexponential decays come from similar relaxation times for the crystalline and amorphous regions. Thus, the same type of motion occurs in both phases where negligible spin diffusion takes place (as confirmed by ²H n.m.r. measurements¹⁷). At low frequencies however, a distinction between amorphous and crystalline motions is available from the $T_{1\rho}$ biexponential decays. According to the f.i.d. deconvolution, the long $T_{1\rho}$ component (intensity of 55%) is related to the motion in the crystalline phase, while the remaining short component is attributed to the amorphous phase. The short $T_{1\rho}$ component arises from a slow modulation of the residual dipolar interaction by the amorphous phase⁸. This confirms the coexistence of two independent processes in the amorphous phase: a slow one and a fast one, the latter also occurring in the crystalline phase.

The effect of pressure on spin-lattice relaxation times consists of a shift to lower temperatures (or lower frequencies). It should be noted that at low frequency a clear decomposition into two components was possible. Whereas for Hirschinger *et al.*⁸, such a numerical decomposition needed an additional constraint, a fixed intensity ratio. Their chosen ratio (0.7) corresponded to an estimated value for the crystalline part, while we found the ratio to be close to 0.55.

Fast anisotropic motion

Since the behaviour of the spin-lattice relaxation times plotted versus $1/T$ in Figures 5 and 6 does not present a minimum over the entire pressure range studied, a direct determination of the correlation time of the motion is

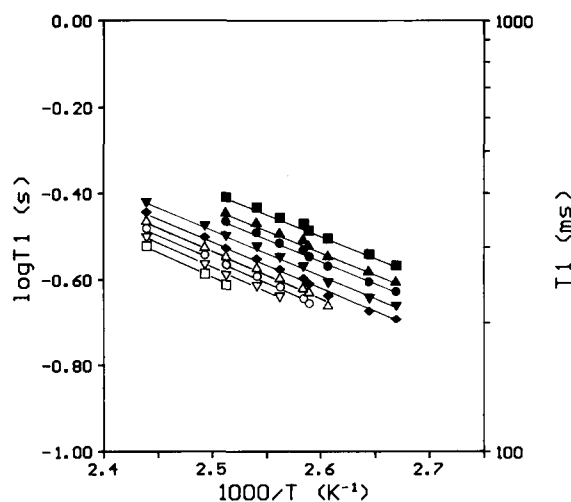


Figure 5 Plot of $\log T_1$ versus $1/T$ at constant pressure. The points have been obtained from the solid line in Figure 2. Pressure (in MPa): (■) 0.1; (▲) 30; (●) 50; (▼) 70; (◆) 100; (△) 120; (○) 140; (▽) 160; (□) 180

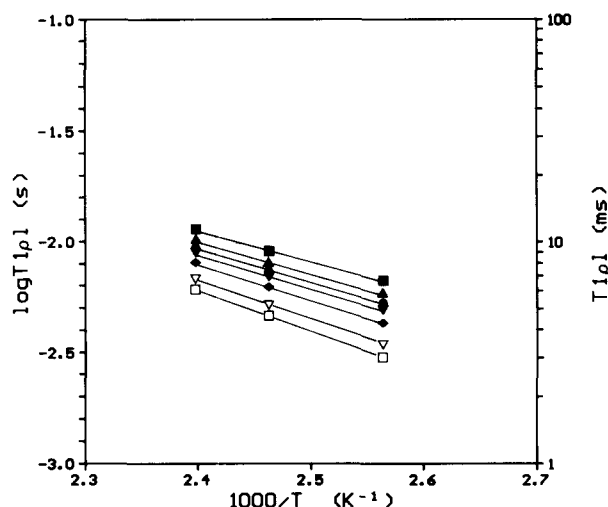


Figure 6 Plot of $\log T_{1\rho 1}$ (11 kHz) long component versus $1/T$ at constant pressure (in MPa): (■) 0.1; (▲) 30; (●) 50; (▼) 80; (◆) 100; (▽) 150; (□) 180

still not possible at high pressure. However, as a large part of the second moment M_2 is modulated by the motion, correlation times of the motion are rather fast. Elsewhere, as plots of $(T_{1\rho})^{-1}$ versus $(\nu_1)^{-1/2}$ (Figure 4) are linear, one can obtain an absolute value in assuming that the spectral density model proposed for the ^1H resonance at different frequencies, $J(\omega) = (\tau_D/\omega)^{1/2}$, is still valid.

The theoretical expressions of spin-lattice relaxation times in the weak collision limit are the following (without transient Overhauser effect⁸):

For T_1^{18} :

$$\frac{1}{T_1} = \frac{2}{3} \Delta M_2^{\text{FF}} [J(\omega_F) + 4J(2\omega_F)] + \frac{1}{2} \frac{N_H}{N_F} \Delta M_2^{\text{HF}} [J(\omega_H - \omega_F) + 3J(\omega_H) + 6J(\omega_H + \omega_F)] \quad (1)$$

For $T_{1\rho}^{19}$:

$$\frac{1}{T_{1\rho}} = \Delta M_2^{\text{FF}} J(2\omega_1) + \frac{N_H}{N_F} \Delta M_2^{\text{HF}} J(\omega_1) + (\omega_1 \text{ independent terms}) \quad (2)$$

where ω_F and ω_H are the Larmor pulsations, respectively, for the ^{19}F and ^1H resonance, ω_1 is the spin-lock pulsation, and ΔM_2^{FF} and ΔM_2^{HF} are, respectively, the homonuclear and heteronuclear second moment that are modulated by the motion.

Since, in the paraelectric phase, no pressure change occurs in the observed second moment (see earlier) and in the chain conformation¹⁴, the previous quantities being of intramolecular origin^{4,8} are also independent of pressure.

Taking the value of ΔM_2^{FF} and ΔM_2^{HF} estimated at atmospheric pressure, the spin-lattice relaxation times can then be related to correlation time through the following expressions:

$$\frac{1}{T_1} = C_{T_1} \left(\frac{\tau_D}{\omega_F} \right)^{1/2} \quad \frac{1}{T_{1\rho}} = C_{T_{1\rho}} \left(\frac{\tau_D}{\omega_1} \right)^{1/2} \quad (3)$$

The factors C_{T_1} and $C_{T_{1\rho}}$ including ΔM_2^{FF} and ΔM_2^{HF} have no pressure dependence. Calculation gives $C_{T_1} = 1.35 \times 10^{10}$ and $C_{T_{1\rho}} = 3.34 \times 10^9 \text{ rad}^2 \text{ s}^{-1/2}$.

From a phenomenological point of view, we assume that the motion is an activated process. The reorientational correlation time is represented in the usual way²⁰ by:

$$\tau_D = \tau_{D_0} \exp\left(\frac{\Delta G^*}{RT}\right) \quad (4)$$

where ΔG^* is the apparent free enthalpy of activation.

We shall discuss below the different assumptions that are often made.

Since C_{T_1} and $C_{T_{1\rho}}$ are pressure independent and assuming also that the pre-exponential term τ_{D_0} has no such dependence (and no temperature variation), we can define ΔH^* , the apparent enthalpy of activation at constant pressure and ΔV^* , the apparent volume of activation at constant temperature by the following equations:

$$\Delta H^* = -R \left[\frac{\delta \ln \tau_D}{\delta(1/T)} \right]_P \quad (5)$$

$$\Delta V^* = -RT \left[\frac{\delta \ln \tau_D}{\delta P} \right]_T \quad (6)$$

(The term entropy of activation, ΔS^* , which is often temperature independent, is included in the pre-exponential term.)

One can obtain ΔV^* from the pressure dependence of $\ln T_1$ (Figures 2 and 3):

$$T_1(T, P) = A(T) \exp\left[-\left(\frac{\Delta V^*}{2RT}\right)P\right] \quad (7)$$

and ΔH^* from Figures 5 and 6, where T_1 and $T_{1\rho}$ are plotted versus $1/T$ at constant pressure (the points are taken from the fitted lines of Figures 2 and 3):

$$T_1(T, P) = B(P) \exp\left(-\frac{\Delta H^*}{2RT}\right) \quad (8)$$

ΔV^* and ΔH^* from T_1 and $T_{1\rho}$ data are reported in Tables 1 and 2 and will be discussed below.

Simple least squares treatment on $A(T)$, $B(P)$, ΔV^* and ΔH^* allowed us to write general expressions for the correlation times as a function of T and P .

From T_1 data:

$$\tau_{D, T_1}(T, P) = 1.23 \times 10^{-16} \exp(-7.52 \times 10^{-3} P) \times \exp[(4.10 \times 10^{-2} P + 38.16)/RT] \quad (9)$$

Table 1 Activation volume at constant temperature from T_1 and $T_{1\rho}$ data as described in the text

T (K)	ΔV^* ($\text{cm}^3 \text{ mol}^{-1}$)	
	T_1	$T_{1\rho}$
374.6	17.2	
386.0	17.9	
390.0		28.4
390.3	17.1	
393.6	17.2	
398.0	17.1	
401.0	17.0	
406.0		24.3
417.0		18.7

Table 2 Activation enthalpy and activation energy defined by $\Delta E^* = \Delta H^* - P\Delta V^*$ at constant pressure from T_1 and $T_{1\rho}$ data

P (MPa)	ΔH^* (kJ mol ⁻¹)		P (MPa)	ΔE^* (kJ mol ⁻¹)	
	T_1	$T_{1\rho}$		T_1	$T_{1\rho}$
0.1	38.6	51.4	0.1	38.9	51.4
30	39.2	53.5	30	38.9	52.7
50	40.2	55.6	50	39.3	54.3
70		58.1	100	40.6	57.7
80	40.9		160	42.1	61.9
100	42.3	60.6	180	42.3	63.1
120	43.1				
140	44.0				
150		65.6			
160	44.9	66.3			
180	45.6	68.1			

From $T_{1\rho}$ data:

$$\tau_{D,T_{1\rho}}(T, P) = 1.83 \times 10^{-17} \exp(-1.92 \times 10^{-2} P) \times \exp[(9.57 \times 10^{-2} P + 51.04)/RT] \quad (10)$$

where T is temperature (in K), P is pressure (in MPa) and the value of the enthalpy is in kilojoules.

At atmospheric pressure, from T_1 , the activation energy and the absolute values of the correlation times are about the same as those determined previously using the ¹⁹F and ¹H resonances⁸ ($\Delta E^* \approx 39$ kJ mol⁻¹ and $\tau_D \approx 15$ ps at 390 K). Correlation times deduced from $T_{1\rho}$ relaxations were about three times higher for the ¹H resonance. One finds that they are seven times greater and the activation energy increases by $\sim 50\%$.

With increasing pressure, correlation times and the enthalpy of activation become greater; and $\tau_{T_{1\rho}}$ seems to be more sensitive to pressure than τ_{T_1} . As at 150 MPa, the ratio of the enthalpies determined from $T_{1\rho}$ and T_1 is of the same order as at atmospheric pressure, the ratio between correlation times ($\tau_{T_{1\rho}}/\tau_{T_1}$) is about 13.5 at 406 K and 17 at 390 K. A difference between $\tau_{T_{1\rho}}$ and τ_{T_1} may only come from a distribution of jump times leading to a distribution of correlation times²¹. Such a ratio could be explained by an increase in the distribution of correlation times with increasing pressure. Alternatively, the one-dimensional fluctuation model⁸ may become progressively less adequate with increasing pressure and decreasing temperature.

One notes otherwise that over the entire pressure and temperature range, the experimental data confirm the existence of a slow motion in the amorphous phase (long tail f.i.d. signal and two components observed for $T_{1\rho}$ at low frequency). However, the data do not give more information than at atmospheric pressure. Correlation times are on a microsecond time-scale.

Activation considerations for the fast anisotropic motion. In principle, a distinction must be made between the experimental quantities ΔH^* and ΔV^* defined by equations (5) and (6) and the theoretical ones ΔH and ΔV related by the thermodynamical equation: $\Delta H = \Delta E + P\Delta V$ (where ΔE is the activation energy and P the external pressure). One can only identify one to another when ΔH^* and ΔV^* are temperature and pressure independent. This is the case when $\ln T_1$ versus $1/T$ on the one hand and $\ln T_{1\rho}$ versus P on the other hand are linear. We shall therefore consider:

$$\Delta H^*(T, P) = \Delta E^*(T, P) + P\Delta V^* \quad (11)$$

Starting from the values of ΔH^* at constant pressure and ΔV^* at constant temperature, our results allow us to estimate the activation energy at constant volume ΔE_v . Such a quantity is of physical importance in the way that it is a measure of constraints to motion other than those involving lattice expansions.

By analogy with equations (5) and (6), in the literature authors usually define an apparent activation energy:

$$\Delta E_v^*(T, V) = -2R \left[\frac{\delta \ln T_1}{\delta(1/T)} \right]_V \quad (12)$$

This quantity is difficult to measure directly, but can be obtained mathematically by:

$$\Delta H^* = \Delta E_v^* + T \left(\frac{\delta P}{\delta T} \right) \Delta V^* = \Delta E_v^* + P_t \Delta V^* \quad (13)$$

P_t is the thermal pressure defined by $P_t = T(\alpha/\chi_T)$, where $\alpha = (1/V)(\delta V/\delta T)_P$ is the thermal expansion coefficient and $\chi_T = -(1/V)(\delta V/\delta P)_T$ is the isothermal compressibility. ΔE^* and ΔE_v^* are related by:

$$\Delta E^*(T, P) = \Delta E_v^*(T, V) + \Delta V^*(T, P) \left[T \left(\frac{\delta P}{\delta T} \right) - P \right] \quad (14)$$

Tables 1 and 2 summarize the activation parameters defined previously. The apparent activation enthalpy (and energy) at constant pressure and volume at constant temperature were found to be $\sim 50\%$ greater from $T_{1\rho}$ than from T_1 . In both cases, ΔH^* (and ΔE^*) increase linearly with pressure (Figure 7). The behaviour of the activation volume is different (Figure 8). As it appears temperature independent from T_1 ($\Delta V^* \approx 17.2$ cm³ mol⁻¹), ΔV^* decreases remarkably from $T_{1\rho}$, with increasing temperature.

In principle, $T_{1\rho}$ measurements probe motions of low frequencies (and large polymer segments). If we assume that ΔV^* reflects the size of the relaxing unit, a difference in ΔV^* derived from T_1 and $T_{1\rho}$ could be expected (as with ΔV^* from viscoelastic measurements or low frequency dielectric relaxations).

It is of interest to compare our values with those found for other polymers. From dielectric studies on linear polyethylene, Sayre *et al.*²² have found $\Delta V^* \approx 18$ cm³ mol⁻¹ at 403 K and Anderson *et al.*²³ reported $\Delta V^* \approx 20$ cm³ mol⁻¹

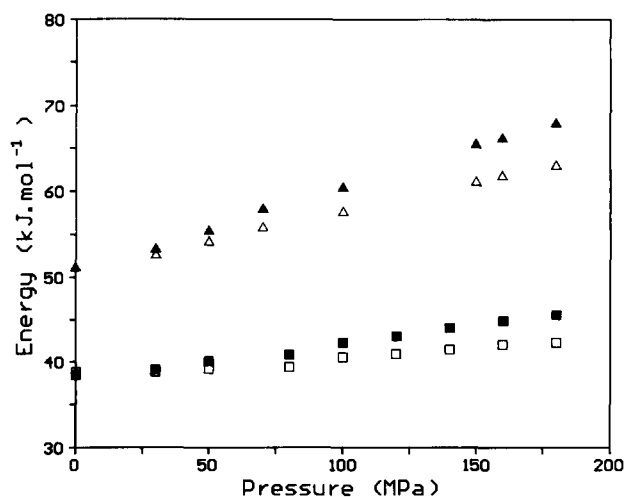


Figure 7 Plots of apparent activation enthalpy ΔH^* (solid symbols) and energy ΔE^* (open symbols) at constant pressure as a function of pressure from T_1 (■, □) and $T_{1\rho}$ (▲, △)

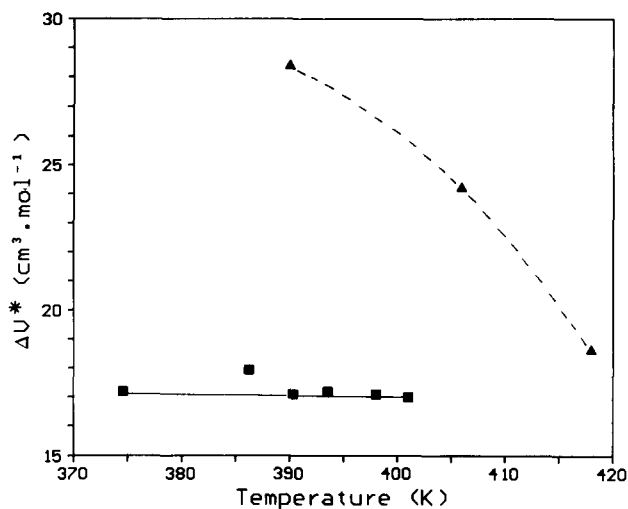


Figure 8 Plots of apparent activation volume ΔV^* as a function of temperature from T_1 (■) and $T_{1\rho}$ (▲) data as described in the text (the lines are to guide the eye only)

(temperature independent) for *cis*-polybutadiene from n.m.r. measurements at high temperature. For the latter, Liu and Jonas²⁴ reported that $\Delta V^*(T_{1\rho})$ decreases with increasing temperature in agreement with dielectric and viscoelastic measurements.

To determine ΔE_v^* according to equation (13), we used the thermodynamic coefficients found by neutron scattering¹⁴ at 390 K in the paraelectric phase: $\alpha = 6.3 \times 10^{-4} \text{ K}^{-1}$ and $\chi_T = 2.5 \times 10^{-10} \text{ Pa}^{-1}$. Activation volumes taken into account were, respectively from T_1 and $T_{1\rho}$, the average value $\Delta V^* \approx 17.2 \text{ cm}^3 \text{ mol}^{-1}$ and $\Delta V^* = 28.4 \text{ cm}^3 \text{ mol}^{-1}$, the value at 390 K.

At this temperature, the ratio $\Delta E_v^*/\Delta H^*$ for our sample range from both T_1 and $T_{1\rho}$ between 0.5 and 0.6 as the pressure increased from 0.1 to 180 MPa. The values found from n.m.r. measurements in polybutadiene are similar: Liu and Jonas²⁴ reported 0.6 and results from Anderson and Slichter²⁵ gave a value of 0.5. These authors mentioned also that this ratio is smaller than the one obtained from dielectric or viscosity measurements. We note that according to references 22, dielectric measurements on polyethylene give a value of 0.76.

Our results indicate that the relaxation times of the VF₂-TrFE copolymer are controlled both by the effects of temperature and volume. Thus, ~40–50% of the mobility increase of segments with increasing temperature under constant pressure results from volume expansion.

CONCLUSIONS

Since the application of hydrostatic pressure can be used to slow molecular motions, the dynamic range of previous

¹H n.m.r. measurements has not been extended. In the paraelectric phase, the pressure range studied is too narrow to show any great modification for T_1 . The highest pressure only results in a doubling of the measuring frequency.

The intramolecular origin assumed for the observed second moments is confirmed by this work. These results are consistent with neutron diffraction results¹⁴: the pressure induced lattice compression induces no change in chain conformation.

ACKNOWLEDGEMENT

We are grateful to R. Hecht for building the high pressure cell.

REFERENCES

- 1 Furukawa, T. *Phase transitions* 1989, **18**, 143
- 2 Tashiro, K., Takano, K., Kobayashi, M., Chatani, Y. and Tadokoro, H. *Polymer* 1984, **25**, 195
- 3 Lovinger, A. J., Furukawa, T., Davis, G. T. and Broadhurst, M. G. *Polymer* 1983, **24**, 1225
- 4 Hirsinger, J., Meurer, B. and Weill, G. *Polymer* 1987, **28**, 721
- 5 Furukawa, T., Ohuchi, M., Chiba, A. and Date, M. *Macromolecules* 1984, **17**, 1384
- 6 Legrand, J. F., Schuele, P. J., Schmidt, V. H. and Minier, M. *Polymer* 1985, **26**, 1683
- 7 Legrand, J. F., Delzenne, P., Dianoux, A. J., Bee, M., Poissonon, C., Broussoux, D. and Schmidt, V. H. *Springer Proc. Phys.* 1988, **29**, 59
- 8 Hirsinger, J., Meurer, B. and Weill, G. *J. Phys. France* 1989, **50**, 583
- 9 Cabarcos, E. L., Arche, A. G., Galleja, F. J. B., Bosecke, P., Rober, S., Bark, M. and Zachmann, H. G. *Polymer* 1991, **32**, 3097
- 10 Akashige, E., Taki, S., Horiuchi, T., Takemura, T. and Matsushige, K. *Rep. Progr. Polym. Phys. Jpn* 1987, **30**, 511
- 11 Matsushige, K., Horiuchi, T., Taki, S. and Takemura, T. *Jpn J. Appl. Phys.* 1985, **24**, 203
- 12 Samara, G. A. *J. Polym. Sci., Polym. Phys. Edn* 1989, **27**, 39
- 13 Huber, H., Mali, M., Roos, J. and Brinkmann, D. *Rev. Sci. Instrum.* 1984, **55**, 1325
- 14 Bellet-Amalric, E., Legrand, J. F., Stock-Schweyer, M. and Meurer, B. *Polymer* in press
- 15 Bourgaux-Leonard, C., Legrand, J. F., Renault, A. and Delzenne, P. *Polymer* 1991, **32**, 597
- 16 Delzenne, P. *PhD thesis* Grenoble University, 1986
- 17 Stock-Schweyer, M., Hirsinger, J., Meurer, B. and Weill, G. in preparation
- 18 Abragam, A. 'The Principles of Nuclear Magnetism', Oxford University Press, New York, 1961
- 19 Stokes, H. T. and Ailon, D. C. *Phys. Rev. B* 1978, **18**, 141
- 20 Glasstone, S., Laidler, K. J. and Eyring, H. 'The Theory of Rate Processes', McGraw-Hill, New York, 1941
- 21 McBrierty, V. J. and Douglas, D. C. *Phys. Rep. (Rev. Sect. Phys. Lett.)* 1980, **63**, 6
- 22 Sayre, J. A., Swanson, S. R. and Boyd, R. H. *J. Polym. Sci., Polym. Phys. Edn* 1978, **16**, 1739
- 23 Anderson, J. E., Davis, D. D. and Slichter, W. P. *Macromolecules* 1969, **2**, 160
- 24 Liu, N. I. and Jonas, J. *J. Magn. Res.* 1975, **18**, 444
- 25 Anderson, J. E. and Slichter, W. P. *J. Chem. Phys.* 1966, **44**, 1797